# First-principles calculations of carrier-doping effects in $SrTiO_3$

Kazuyuki Uchida* and Shinji Tsuneyuki
*Department of Physics, University of Tokyo, 7-3-1 Hongo Bunkyo-ku, Tokyo 113-0033, Japan*

Tatsuo Schimizu
*Advanced LSI Technology Laboratory, R&D Center, Toshiba Corporation 1, Komukai Toshiba-cho, Saiwai-ku, Kawasaki 212-8582, Japan*

(Received 14 April 2003; revised manuscript received 10 September 2003; published 20 November 2003)

Carrier-doping effects on the structural phase transitions in $SrTiO_3$ are investigated by the first-principles calculations. It is found that the instabilities of the cubic phase to both the $TiO_6$-octahedron rotated phase and the ferroelectric phase are modulated characteristically by the electron doping and the hole doping. The results of the calculations are consistent with a previous experiment in which carrier electrons were introduced by impurity doping, and with another experiment where carriers were doped in $SrTi^{18}O_3$ by photo-irradiation. The modulations of the instabilities are explained by a simple and intuitive mechanism.

DOI: 10.1103/PhysRevB.68.174107 PACS number(s): 77.80.Bh, 77.84.Dy

## I. INTRODUCTION

Structural phase transitions in $SrTiO_3$ attract a great deal of attention due to their isotope effects.[1,2] Experimentally, the cubic phase structure is found at high temperatures, while the $TiO_6$-octahedron rotated phase is observed below 105 K in $SrTi^{16}O_3$ and below 110 K in $SrTi^{18}O_3$ (Fig. 1). Judging from the fact that the ferroelectric phase is not observed in $SrTi^{16}O_3$ but found only in $SrTi^{18}O_3$ below 23 K, it is insisted that $SrTi^{16}O_3$ is a quantum paraelectric material[3] in which zero-point oscillation and tunneling effect of the atomic nuclei prevent the ferroelectric phase from appearing even at 0 K. Barrett's analytical formulation on the characteristic behavior of the dielectric constant also supports this hypothesis.[3]

Recently, Takesada *et al.*[2] suggested a possibility of the photoinduced ferroelectric transition of $SrTi^{16}O_3$ from their experiments. Since $SrTi^{18}O_3$ does not show this effect at all, the photoinduced ferroelectric transition is also thought to be concerned with the quantum effects of nuclei. A previous impurity-doping experiment[4] in $SrTi^{16}O_3$ showed suppression of the ferroelectric instability by the doped electrons. The different effects of carriers between the impuritydoping and the photodoping are also worth inquiring.

Looking from the practical point of view, the photoinduced ferroelectric transitions in dielectric materials have a wide range of applications. Dielectric thin films which are applied in the electrical circuits on semiconductors can be developed as photoelectronic elements, for example. Photoswitched capacitors, devices, and memories would be developed in the future. The photoinduced ferroelectric transition is theoretically interesting, too, because it suggests a possibility of controlling the quantum fluctuation by an external perturbation.

In this paper, we investigate the carrier-doping effects in $SrTiO_3$ by the first-principles calculations. The modulations of not only the ferroelectric instability but also the $TiO_6$-octahedron rotating instability by the doped carriers are simulated in agreement with experiments, except for the photodoping effect on the ferroelectric instability in $SrTi^{16}O_3$. The modulations of the instabilities are explained by a simple and intuitive mechanism.

## II. METHOD OF CALCULATIONS

### A. First-principles calculations

First-principles calculations based on the density-functional theory (DFT) and local-density approximation (LDA) is a powerful tool which has succeeded in describing not only the structural stabilities but also the electronic and mechanical properties of so many systems without depending on any empirically determined parameters. Since Co-

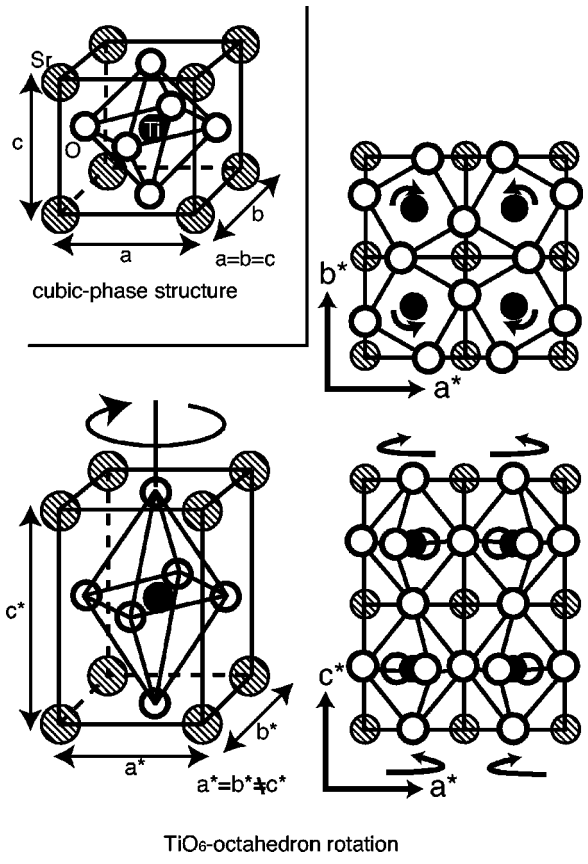


FIG. 1. The cubic phase structure and the $TiO_6$-octahedron rotated structure are shown. The unit cell of the cubic phase is composed of five atoms, while that of the $TiO_6$-octahedron rotated phase consists of ten atoms.

 

TABLE I. The lattice constant and the bulk modulus of the cubic-phase structure are shown. The first-principles calculations can reproduce the experimental results within very small error. It is known that the difference of the lattice constant between $SrTi^{16}O_3$ and $SrTi^{18}O_3$ is exceedingly small (within the range of the experimental error).[1]

| | Experiment | This work |
|---|---|---|
| Lattice constant | 7.394 a.u.[a] | 7.342 a.u. (−0.7%) |
| Bulk modulus | 183 GPa[b] | 19 4GPa (+6%) |

[a]Reference 15.
[b]Reference 16.

hen's advanced work,[5,6] the electronic structures and the structural phase transitions of many dielectric materials have also been studied by the method of the first-principles calculations. The typical perovskite-type titanium oxides such as $SrTiO_3$,[7–10] $BaTiO_3$,[5,10–12] and $PbTiO_3$,[5,6] have been investigated especially vigorously. The problem of the double structural instabilities (the $TiO_6$-octahedron rotation and the ferroelectric displacement)[7,8] and the quantum paraelectricity[9,10] in $SrTiO_3$ attracts a great deal of attention, which has also been studied successfully with the aid of the first-principles calculations. We can expect the accuracy and reliability of the results of our calculations in the study of the carrier-doping effects on the structural phase transitions in $SrTiO_3$.

In this work, the exchange-correlation energy of the PZ81-type[13] and the Vanderbilt's ultrasoft pseudopotential method[14] were adopted. The cutoff energy of the plane waves to expand the one-electron wave functions was chosen at 49 Ry. 125 reducible *k* points were sampled in order to reproduce the experimental lattice constant and the bulk modulus of the cubic phase within very small error (Table I). We also succeeded in reproducing the structural parameters of the $TiO_6$-octahedron rotated phase at the energy of dozens of meV lower than the cubic phase (Table II).

For calculating the photo-carrier (electron-hole pair)-doped states, we performed an irregular way of filling up the Kohn-Sham orbitals, i.e., the one-electron wave functions: the top of the valence band was left empty by a fixed amount, while the bottom of the conduction band was filled by the same amount of electrons through the iterations for obtaining the self-consistent field. Previous calculations,[17,18] which succeeded in describing the experimentally predicted photoexcited electronic states (excitons) in insulators support the validity of adopting formally the same density functional as that for the nonexcited electronic states. No spin polarization was assumed in our calculations.

TABLE II. The lattice and structure parameter of the $TiO_6$-octahedron rotated phase is shown. Our calculation reproduces the results of experiments at least qualitatively.

| | $a^*=b^*$ | $c^*/a^*$ | Rotation |
|---|---|---|---|
| Experiment[a] | 0.9944 | ~1 | 2.1° |
| This work | 0.9988a | ~1 | 8.4° |

[a]Reference 15.

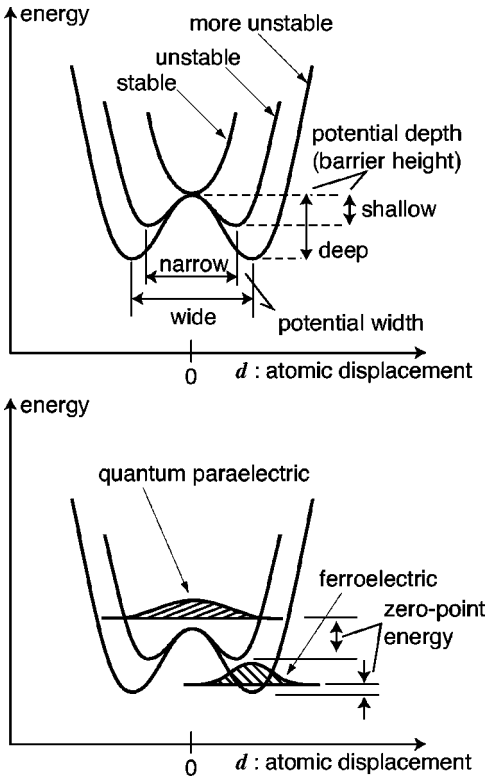


FIG. 2. Upper: The adiabatic potential energy surfaces are drawn without considering the quantum effects of nuclei. *d* means the schematic atomic displacement, i.e., the rotation of the $TiO_6$-octahedron or the ferroelectric displacement. Lower: The ground states are drawn to evaluate the quantum effects of nuclei. The ferroelectric instability in $SrTi^{16}O_3$ is extinguished when considering the quantum effect (quantum paraelectric state). The deeper and the wider the double-minimum potential is, the larger instability is expected due to the higher potential barriers and the smaller zero-point energy of the atomic oscillations.

### B. Evaluation of the instabilities

The adiabatic energy potential surfaces of the system for the $TiO_6$-octahedron rotation and the ferroelectric displacement (schematically represented by *d*) with respect to the cubic phase structure are drawn without considering quantum effects of nuclei explicitly (Fig. 2). Reflecting the energetic instability of the cubic phase structure, the double-minimum-type potential is obtained. The deeper and wider the double-minimum potential is, the larger instability, i.e., the higher phase-transition temperature and the larger atomic displacements, is expected. As $SrTiO_3$ is a quantum paraelectric material, the zero-point oscillation energy of nuclei must be evaluated in order to take account of the quantum effect of nuclei which tends to prevent the system from being trapped at the potential minimum. In the following calculations, however, the deeper potential is always wider than the shallower one, being accompanied by smaller zero-point oscillation energy. Therefore, the relative strength of the structural instabilities between two potentials is qualitatively in-

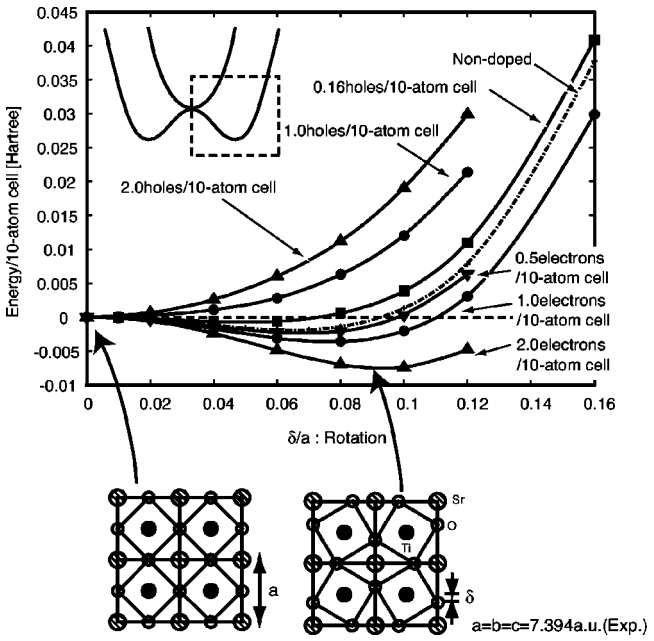


FIG. 3. The carrier-doping effect on the $TiO_6$-octahedron rotating instability is presented. The doped electrons lead to the increase of the $TiO_6$-octahedron rotating instability, while the doped holes bring about the decrease of the instability. The lattice constant is fixed at the experimental value.

variant even if the quantum effect of nuclei is considered. Such being the case, we can solve the problem of the carrier-doping dependence of the structural instabilities without considering the quantum effect of nuclei explicitly in the following arguments.

## III. RESULTS AND DISCUSSIONS

The doped-carrier density in experiments is at most $\sim 0.001$ carriers/unit cell. We confirmed that the variation of the lattice constant by them is exceedingly small, which affect neither the $TiO_6$-octahedron rotating instability nor the ferroelectric instability. In the following calculations, the cell parameters were fixed at the experimental value of the cubic phase, $a = 7.394$ a.u. The degrees of the $TiO_6$-octahedron rotation and the ferroelectric displacement are represented by the displacement of an O atom divided by $a$ (see Fig. 3 and Fig. 7).

### A. Carrier-doping effects on the $TiO_6$-octahedron rotation

The calculated electron-doping effect and the hole-doping effect on the $TiO_6$-octahedron rotating instability are shown in Fig. 3. As is already explained, the wider and the deeper the double-minimum potential is, the larger instability is expected. The electron doping gives rise to the increase of the $TiO_6$-octahedron rotating instability, bringing about the larger rotation angle and the higher phase-transition temperature than the undoped case. On the contrary, the hole doping leads to the suppression of this instability, resulting in the smaller rotation angle and the lower phase-transition temperature.

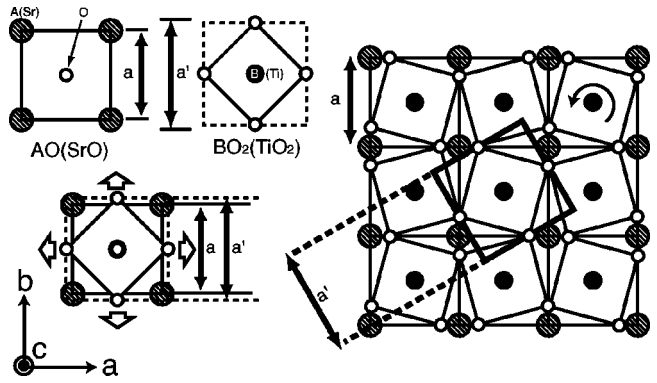


FIG. 4. The origin of the $BO_6$-octahedron rotating instability is explained. The disagreement between the sizes of the $AO$ square ($a$) and that of the $BO_2$-square $a'$ is the origin of the rotation. In order to fit the large $BO_2$ square ($a'$) in the small $AO$ square ($a$), the $BO_6$-octahedron rotates around the $c$ axis. The expansion of the $BO_2$ square (white arrows) will bring about larger rotation of the $BO_6$ octahedron. $a=\sqrt{2}(r_A+r_O)$ and $a'=2(r_B+r_O)$, where $r_A$, $r_B$, and $r_O$ are ionic radii of each ion.

A previous impurity-doping experiment[4] showed that the doped electrons do not affect the $TiO_6$-octahedron rotating instability. We confirmed that the low-density doping as the experiment ($\leqslant 0.001$ electrons/10-atoms cell) brings about an effect too small to be observed experimentally, which means that our calculation is consistent with the experiment.

The concept of "*tolerance factor*" (Ref. 19) is useful for understanding the $TiO_6$-octahedron rotation. The tolerance factor of a perovskite compound $ABO_3$, $t$, is defined as the ratio of the intrinsic sizes of the $AO$ square $a$ and the $BO_2$ square $a'$:

$$t=\frac{a}{a'}=\frac{r_A+r_O}{\sqrt{2}(r_B+r_O)}. \tag{1}$$

$r_A$, $r_B$, and $r_O$ are ionic radii of each ion (see Fig. 4). The strong correlation between the $BO_6$-octahedron rotating instability and the tolerance factor has been confirmed as to a series of $ABO_3$'s:[20] the smaller the tolerance factor is, the larger the rotating instability is.

The fact that $TiO_2$ square is larger than the SrO square (i.e., $t$ is smaller than 1) is the origin of the rotation of the $TiO_6$-octahedron in $SrTiO_3$. In order to fit the large $TiO_2$ square in the small SrO square, the $TiO_6$-octahedron rotates around the $c$ axis. The variation of the tolerance factor means that of the ratio of the square sizes and brings about the modulation of the $TiO_6$-octahedron rotating instability.

The carrier doping gives rise to the variation of the ionic radii and that of the tolerance factor, leading to the modulation of the $TiO_6$-octahedron rotating instability according to the argument above. To know the carrier-doping effects on the ionic radii, the analysis of the top of the valence band and the bottom of the conduction band on the component is essential. As shown in Fig. 5, the bottom of the conduction band of $SrTiO_3$ is composed of Ti-3$d$ orbitals, while the top of the valence band consists of O-2$p$ orbitals. The doped electrons accommodated in the Ti-3$d$ orbitals increase the

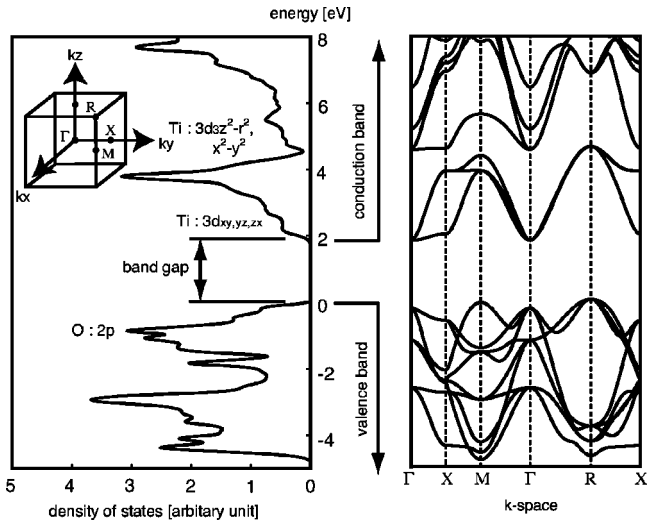


FIG. 5. The band structure and the density of states of the cubic phase of $SrTiO_3$ is shown. $SrTiO_3$ is a insulator with a band gap width of 1.89 eV (smaller than the experimental value of 3.2 eV because of LDA). The top of the valence band is composed of O:$2p$ orbitals, while the bottom of the conduction band consists of Ti:$3d$ orbitals. Sr:$5s$ band is located at higher energy than these bands. The electron doping and the hole doping are not directly related to Sr:$5s$ orbitals.

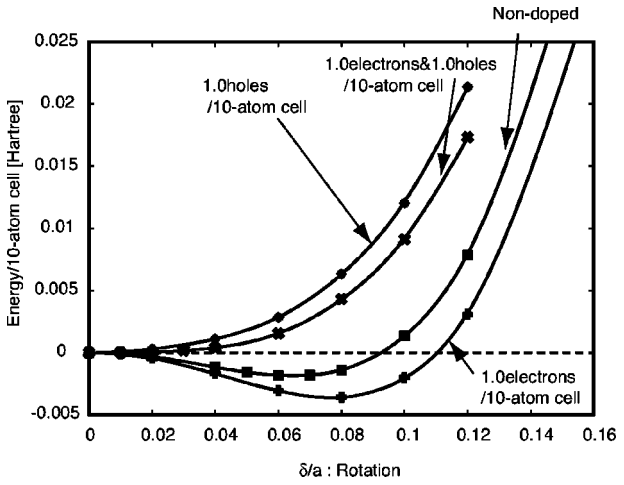


FIG. 6. The electron-hole-pair doping effect on the $TiO_6$-octahedron rotating instability is shown. The result can be interpreted as the superposition of the effects of the doped electrons and the doped holes. The suppression of the $TiO_6$-octahedron rotating instability by the doped holes exceeds the promotion of the instability by the same amount of doped electrons. The lattice constant is fixed at the experimental value. The meaning of the $x$ axis is the same as that of Fig. 3.

electron clouds around the Ti atom, expanding the radius of the Ti ion. The larger radius of the Ti ion leads to the smaller tolerance factor, and therefore to the promotion of the $TiO_6$-octahedron rotating instability.

On the other hand, the doped holes captured at the O-$2p$ orbitals lead to the decreased electron clouds around the O atoms, and therefore to the shrunk radius of the O ion. As

$$t=\frac{r_{\mathrm{Sr}}+r_{\mathrm{O}}}{\sqrt{2}(r_{\mathrm{Ti}}+r_{\mathrm{O}})}=\frac{1}{\sqrt{2}}\left(1+\frac{r_{\mathrm{Sr}}-r_{\mathrm{Ti}}}{r_{\mathrm{Ti}}+r_{\mathrm{O}}}\right) \tag{2}$$

and $(r_{\mathrm{Sr}}-r_{\mathrm{Ti}})$ is positive, the smaller $r_{\mathrm{O}}$ results in the larger tolerance factor, and therefore in the suppression of the $TiO_6$-octahedron rotating instability.

We explained the promotion and suppression of the $TiO_6$-octahedron rotating instability by the expansion and the shrinking of the radii of the ions by the electron doping and the hole doping, respectively.

The systems doped with electron-hole pairs were also calculated in order to investigate the photocarriers doping effect on the $TiO_6$-octahedron rotating instability (Fig. 6). As we expected, the result can be interpreted as the superposition of the effects of the doped electrons and the doped holes, which means that the explanation by the variation of the ionic radii is also applicable to the case of the electron-hole-pair doping, and that the suppression of the $TiO_6$-octahedron rotating instability by the doped holes exceeds the promotion of the instability by the same amount of doped electrons.

### B. Carrier-doping effects on the ferroelectric instability

The electron-doping effect and the hole-doping effect on the ferroelectric instability are shown in Figs. 7 and 8, respectively. Contrary to the carrier-doping effect on the $TiO_6$-octahedron rotating instability, not only the hole doping but also the electron doping give rise to the suppression of the ferroelectric instability. The variation of the ionic radii cannot explain this tendency. The carrier-doping effects on the ferroelectric instability can be explained by considering another side of the variation of the ionic-valence number, i.e., the gain and loss of the electric charges of the Ti ion and

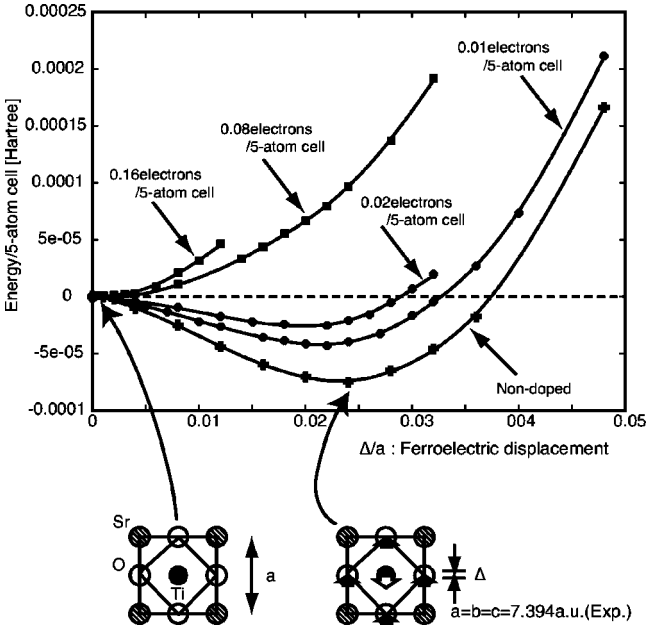


FIG. 7. The electron-doping effect on the ferroelectric instability is drawn. The doped electrons give rise to the suppression of the ferroelectric instability. The lattice constant is fixed at the experimental value.

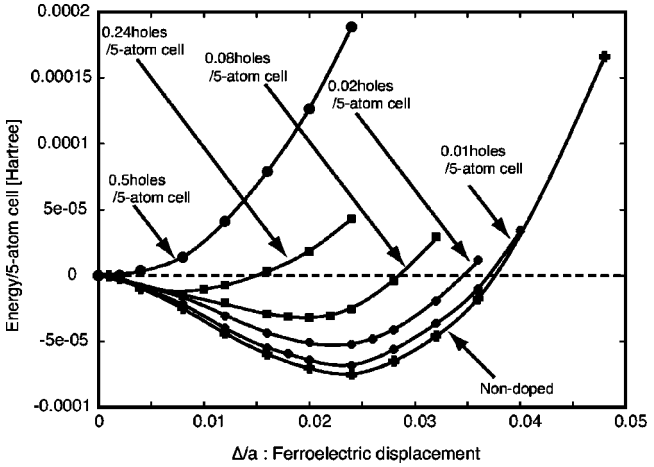


FIG. 8. The hole-doping effect on the ferroelectric instability is presented. Similar to the electron-doping case, the doped holes give rise to the suppression of the ferroelectric instability. The lattice constant is fixed at the experimental value. The meaning of the *x* axis is the same as that of Fig. 7.

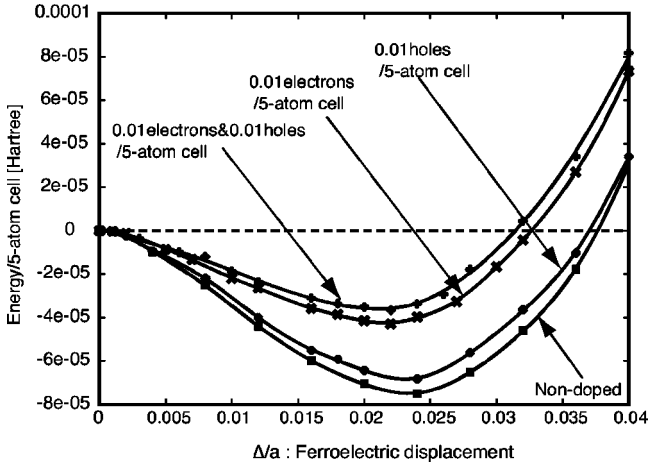


FIG. 9. The electron-hole-pair doping effect on the ferroelectric instability is presented. The result can be interpreted as the superposition of the effects of doped electrons and doped holes. The suppression of the ferroelectric instability by the doped electron-hole pairs is expected, which accounts for the experiment in $SrTi^{18}O_3$. The meaning of the *x* axis is the same as that of Fig. 7.

the O ion. The variation of the electric charges of the ions are not so important in the $TiO_6$-octahedron rotation because it is not accompanied by electric polarizations, while the ferroelectric instability is substantially affected by them due to the fact that the ferroelectric phase is essentially the cooperative phenomenon, stabilized by the long-range Coulomb interactions among the electric dipole moments spontaneously appearing in each cell. As is already explained, the doped electrons are captured at the Ti ions, reducing the positive electric charge of the ions: $Ti^{4+} \rightarrow Ti^{(4-\alpha)+}$, while the doped holes are accommodated at the O ions, diminishing the negative electric charge of the ions: $O^{2-} \rightarrow O^{(2-\beta)-}$. Smaller electric charges lead to smaller electric dipole moments when displaced by the same distance, giving rise to smaller energy gain by Coulomb interactions among them, and therefore to the suppression of the ferroelectric instability.

The impurity-doping experiment[4] showed that the doped electrons suppress the ferroelectric instability. Our results and explanation are consistent with this experiment. Compared with the effect of the doped carriers on the $TiO_6$-octahedron rotating instability, even much smaller amount of carriers seem to be effective enough to modulate the instability. The energy scale of the ferroelectric instability smaller than that of the $TiO_6$-octahedron rotating instability might explain this difference. The electrons captured at the O ion or the Sr ion, or the holes taken in at the Ti ion or the Sr ion would come to quite different results. Here again, the analysis on the component of the top of the valence band and the bottom of the conduction band is important in understanding the carrier-doping effects.

We also performed the calculations on the electron-hole-pair doping effect on the ferroelectric instability (Fig. 9). The doped electron-hole pairs suppress the ferroelectric instability, as is expected from the variations of the electric charges of the ions. The result is also understandable as the superposition of the electron-doping effect and the hole-doping effect. The photocarrier doping experiment in $SrTi^{18}O_3$ (Ref. 2) is consistent with our result.

On the other hand, the present result cannot explain the enhancement of the ferroelectric instability in $SrTi^{16}O_3$ by the photocarriers.[2] Our failure might be concerned with the localized phenomena of carriers which are not treated in this work. For example, a self-trapped exciton in $SrTiO_3$, which is suggested by another experiment,[21] might act as a kernel of the ferroelectric instability[22] through the Jahn-Teller effect. It should be mentioned that, in any case, we have to deal with the quantum effect of nuclei precisely to understand the large difference between $SrTi^{16}O_3$ and $SrTi^{18}O_3$.

## IV. CONCLUSION

The carrier-doping effects in $SrTiO_3$ were examined by first-principles calculations and explained by the simple and intuitive mechanisms. Both aspects of the variation of the ionic-valence number, i.e., the change of the ionic radius and the electric charge, are important in the modulation of the $TiO_6$-octahedron rotating instability and the ferroelectric instability, respectively. The analysis of the top of the valence band and the bottom of the conduction band on the atomic-orbital component helps us to understand the carrier-doping effects on the ionic-valence numbers. The results of our calculations are summarized in Table III.

We found that the rotation of the $TiO_6$-octahedron is promoted by doping electrons, while the hole-doping suppresses the rotation. The rotation of the $TiO_6$ octahedron is induced by the size disagreement between the $TiO_2$ square and the SrO-square. The opposite results of the doping effects between the electron doping and the hole doping is explained by considering the expansion and the shrinking of the radii of the Ti ion and the O ion, and therefore the variation of the ratio of the sizes of the SrO square and the $TiO_2$ square brought about by them. We pointed out that the modulation

TABLE III. The results of our calculations are summarized. The carrier-doping effects on both the instabilities are simulated in agreement with experiments, except for the electron-hole-pair doping effect on the ferroelectric instability in $SrTi^{16}O_3$. The modulations of the instabilities by the carrier doping are explained by a simple and intuitive mechanism.

| | Rotation | Ferroelectricity | |
|---|---|---|---|
| Electron Doping | Promotion | Suppression | Consistent with experiments. |
| Hole Doping | Suppression | Suppression | Theoretical prediction. |
| Electron-Hole-Pair Doping | Suppression | Suppression | Consistent with experiments except for the effect on the ferroelectricity in $SrTi^{16}O_3$. |
| Mechanism | Radii of ions | Electric charges of ions | |

of the $TiO_6$-octahedron rotating instability is, however, too small to be experimentally observed when doped by $\leqslant 0.001$ electrons/10-atoms cell, which is consistent with the previous experiment.

On the other hand, ferroelectric instability of the system is suppressed by both kinds of carrier doping. The ferroelectric phase is stabilized by the cooperative interactions among the electric-dipole moments appearing in each cell. In order to realize the mechanism of the suppressions, consideration on the variation of the electric charges of the ions is essential. The reduced electric-charges by the doped carriers lead to the diminished electric-dipole moments and therefore the decreased energy gain by the long-range Coulomb interactions among them, resulting in the suppression of the ferroelectric instability.

For both the instabilities, the calculated electron-hole-pair doping effect on the instabilities are understandable as the superposition of the effect of the only-electron doping and that of the hole-doping alone. Due to the fact that no hole-doping experiments have been performed yet, our calculations on the hole-doping effects are the first theoretical predictions as far as we know.

The previous impurity-doping experiment[4] showing the reduction of the ferroelectric instability by the doped electrons is consistent with the present results. The photodoping experiments[2] showing the suppression of the ferroelectric instability by the photocarriers in $SrTi^{18}O_3$ is also in harmony with our results, while the photoinduced gigantic dielectric effect in $SrTi^{16}O_3$, which suggests the possibility of the photoinduced ferroelectric transition of the quantum paraelectric material, seems contrary to our calculation. The reason why we failed to explain only the photoinduced gigantic dielectric effect in $SrTi^{16}O_3$ is expected to be concerned with the localization of the doped carriers which was not considered in this work. The localization of the doped carriers, the carrier-lattice interactions, and the quantum effect of the nuclei which is expected to affect them are now under investigation.

## ACKNOWLEDGMENTS

We wish to acknowledge Dr. S. Kimura, Dr. T. Kimura, Dr. K. Akagi, and Dr. Y. Yoshimoto for stimulating and valuable discussions. The theoretical calculation was performed with Tokyo Ab initio Program Package (TAPP), which has been developed by our group.[23,24]

*Electronic address: kuchida@cms.phys.s.u-tokyo.ac.jp

[1] M. Itoh, R. Wang, Y. Inaguma, T. Yamaguchi, Y-J. Shan, and T. Nakamura, Phys. Rev. Lett. **82**, 3540 (1999).
[2] M. Takesada, T. Yagi, M. Itoh, and S. Koshihara, J. Phys. Soc. Jpn. **72**, 37 (2003).
[3] J.H. Barrett, Phys. Rev. **86**, 118 (1952).
[4] H. Uwe and T. Sakudo, Ferroelectrics **52**, 205 (1983).
[5] R.E. Cohen and H. Krakauer, Phys. Rev. B **42**, 6416 (1990).
[6] R.E. Cohen, Nature (London) **358**, 316 (1992).
[7] C. Lasota, C.Z. Wang, R.C. Yu, and H. Krakauer, Ferroelectrics **194**, 109 (1997).
[8] N. Sai and D. Vanderbilt, Phys. Rev. B **62**, 13 942 (2000).
[9] W. Zhong and D. Vanderbilt, Phys. Rev. Lett. **74**, 2587 (1995).
[10] W. Zhong and D. Vanderbilt, Phys. Rev. B **53**, 5047 (1996).
[11] W. Zhong and D. Vanderbilt, Phys. Rev. Lett. **74**, 2587 (1995).
[12] W. Zhong, D. Vanderbilt, and K.M. Rabe, Phys. Rev. B **52**, 6301 (1995).
[13] J.P. Perdew and A. Zunger, Phys. Rev. B **23**, 5048 (1981).
[14] D. Vanderbilt, Phys. Rev. B **41**, 7892 (1990).
[15] T. Ikeda, T. Kobayashi, M. Takata, T. Takayama, and M. Sakata, Solid State Ionics **108**, 151 (1998).
[16] Landolt and Bornstein, *Numerical Data and Functional Relations in Science and Technology–Crystal and Solid State Physics* (Springer-Verlag, Berlin, 1982).
[17] J. Song, H. Jonsson, and L.R. Corrales, Nucl. Instrum. Methods Phys. Res. B **166–167**, 451 (2000).
[18] V. Perebeinos, P.B. Allen, and M. Weinert, Phys. Rev. B **62**, 12 589 (2000).
[19] Y. Xu, *Ferroelectric Materials and Their Applications* (North-Holland, Amsterdam, 1991).
[20] W. Zhong and D. Vanderbilt, Phys. Rev. Lett. **74**, 2587 (1995).
[21] T. Hasegawa, M. Shirai, and K. Tanaka, J. Lumin. **87–89**, 1217 (2000).
[22] J. Shibata and T. Ogawa (private communications).
[23] M. Tsukada *et al.*, computer code TAPP (University of Tokyo, Tokyo, Japan, 2003).
[24] J. Yamauchi, M. Tsukada, S. Watanabe, and O. Sugino, Phys. Rev. B **54**, 5586 (1996).